Supplementary Information

Bimodal "matrix-free" polymer nanocomposites

Ying Li, Lei Wang, Bharath Natarajan, Peng Tao, Brian C. Benicewicz, Chaitanya Ullal, and Linda S. Schadler*

ZrO_2 nanoparticle size distribution was characterized by measuring at least 200 particles using Image J. All the diffraction peaks in the XRD pattern of as-synthesized ZrO_2 nanoparticles (NPs) can be assigned on the basis of a cubic structure (JCPDS, 49-1642)[1], and the size of the nanocrystal was estimated to be 1.9 nm in radius.

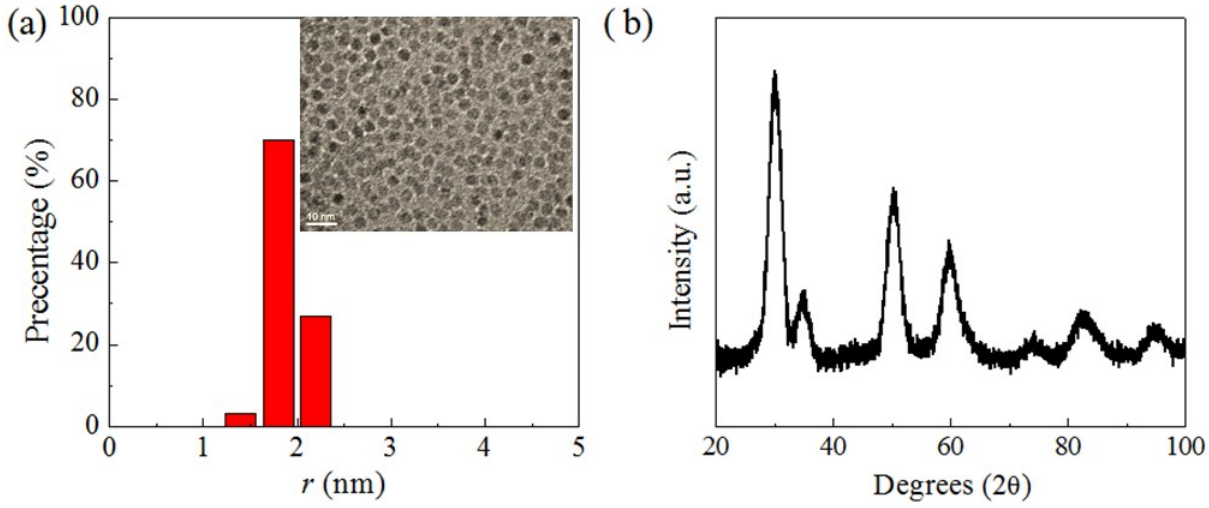

Figure S1. (a) TEM image and size distribution of the as-synthesized ZrO_2 nanoparticles and (b) XRD pattern.

The as-synthesized nanoparticle suspension in chloroform solution appears to be slightly cloudy due to the relatively weak stabilizing effect of benzyl alcohol, which acts as both solvent and stabilizing agent during the nanoparticle synthesis.[2] The chemisorbed benzyl alcohol can be readily replaced by the carboxyalkyl- and phosphate-terminated PDMS brushes, and monomodal, bimodal, and trimodal PDMS grafted nanoparticles, ZrO_2_1k,

ZrO_2_1k_10k, and ZrO_2_1k_36k_10k, respectively, named according to the molecular weight of the brushes, were prepared via multiple-step "grafting-to" processes.

The successful attachment of the PDMS brushes was verified by FTIR spectra, as shown in Figure S2 (a), which were normalized based on the Zr-O-Zr vibrational bands at 450-600 cm^{-1}.[3, 4] For the as-synthesized nanoparticles, the FTIR peaks at 3028 cm^{-1} (C-H stretching vibration of phenyl groups) and 700 cm^{-1} (out-of-plane C-H vibration of phenyl groups) confirmed the presence of the surface-complexing benzoate species after synthesis.[2, 5] The FTIR spectrum of ZrO_2_1k sample displays strong characteristic Si–O stretching vibrations at 1000–1100 cm^{-1}, as well as symmetric and asymmetric vibration of the carboxylate group at 1413 and 1558 cm^{-1} respectively, indicating the chemical interaction between the 1k carboxyalkyl-terminated PDMS brush and surface Zr centers.[5] The strong peaks from 2965 to 2847 cm^{-1} can be attributed to the stretching vibrations of the CH_2 and CH_3 groups of the brush chain.[6] For the ZrO_2_1k_36k_10k sample, the phosphorus characteristic peaks cannot be distinguished probably because the absorption bands of P-O and P=O stretching (900-1300 cm^{-1}) were masked by vibration bands of Si–O and Si–CH_3 from the PDMS brushes.[6, 7] The stretching band at 1728 cm^{-1} in the ZrO_2_1k sample implies residual unbound carboxylic acid groups, which were washed away or replaced by phosphate-terminated PDMS brushes in the ZrO_2_1k_36k_10k sample.

The ligand exchange process agrees well with the TGA weight loss measurement, where the adsorbed hydroxyl and organic volatiles correspond to the weight loss stage at ~300°C, and chemically bound brushes are attributable to the second weight loss stage above 450°C. As shown in Figure S2 (b), the core weight fractions of ZrO_2_1k, ZrO_2_1k_10k, and ZrO_2_1k_36k_10k nanoparticles were also estimated as 79 wt%, 53 wt%, and 44 wt%, respectively. To give a quantitative description of grafted nanoparticle dimensions and architecture, the graft density of each PDMS brush was calculated first based on the

corresponding weight loss ratio and the number of grafting chains (determined by TGA after each step of "grafting-to"), and surface area of nanoparticles using:[8]

$$\sigma = \left(wN_A/M_n\right)/\left(4\pi a^2 n\right) = a\rho z N_A \times 10^{-21}/3(1-z)M_n$$

where w, N_A, n, ρ and z are the weight of polymers, Avogadro's number, the number of nanoparticles, density of nanoparticle cores, and weight loss of polymer chains, respectively. Both as-synthesized and grafted nanoparticles after each step of "grafting-to" were monitored by TGA measurements. To form a stronger P-O-M (M: Metal atom) bond, the 1k carboxyalkyl-terminated PDMS brush grafted on the ZrO_2 nanoparticle surface can be replaced by the 36k and 10k phosphate-terminated PDMS in the sequential "grafting-to" reactions. To estimate the amount of removed 1k brush, ZrO_2_1k nanoparticles were excessively washed using methanol and then subjected to TGA measurement, where ~3 wt% weight loss of 1k brush was observed. The graft densities of each PDMS brush are calculated and listed in Table S1.

Table S1 Graft densities and core percentages of three types of PDMS-grafted ZrO_2 nanoparticles.

Sample	σ_{1k} (ch/nm^2)	σ_{10k} (ch/nm^2)	σ_{36k} (ch/nm^2)	Core percentage (%)
Monomodal ZrO_2	0.28	-	-	79
Bimodal ZrO_2	0.20	0.10	-	53
Trimodal ZrO_2	0.12	0.05	0.02	44

To determine the conformation of grafted PDMS chains, radius of gyration of PDMS polymer chains is calculated using[9] $R_g = \sqrt{0.077 \times N_{PDMS}}$ (nm), and compared with the interchain spacing on the nanoparticle surface in Table S2. At low enough molecular weight or low enough graft density, $\sigma < 1/R_g^2$, individual chains take mushroom-like conformations on the grafting surface with a thickness of radius of gyration. [10, 11] According to simulation studies, the addition of a longer brush population at a low graft density has little impact on the conformation of the inner brushes, and they behave similar to their monomodal counterparts.[12]

Table S2. Parameters used for estimating dimensions of PDMS-grafted nanoparticles.

Polymer chains	N	R_g (nm)	$1/R_g^2$	r/R_g
1k PDMS	14	1.02	0.96	1.9
10k PDMS	135	3.23	0.10	0.59
36k PDMS	486	6.12	0.03	0.31

Given the small radius ratio of "bare" nanoparticle and polymer brush coil ($u = r/R_g < 1$), it is difficult for the 10k and 36k PDMS brushes to fit into the interstitial space between nanoparticles. On the other hand, from a packing point of view, the 1k PDMS brush population fills the interstitial spacing more readily at its size ratio ($u = 1.9 > (\sqrt{3} - 1)^{-1}$).[13]

After careful solvent removal, the grafted nanoparticle assembles remains highly transparent, indicating uniform dispersion and distribution of nanoparticle cores within the PDMS brush polymer, as shown in Figure S2 (c).

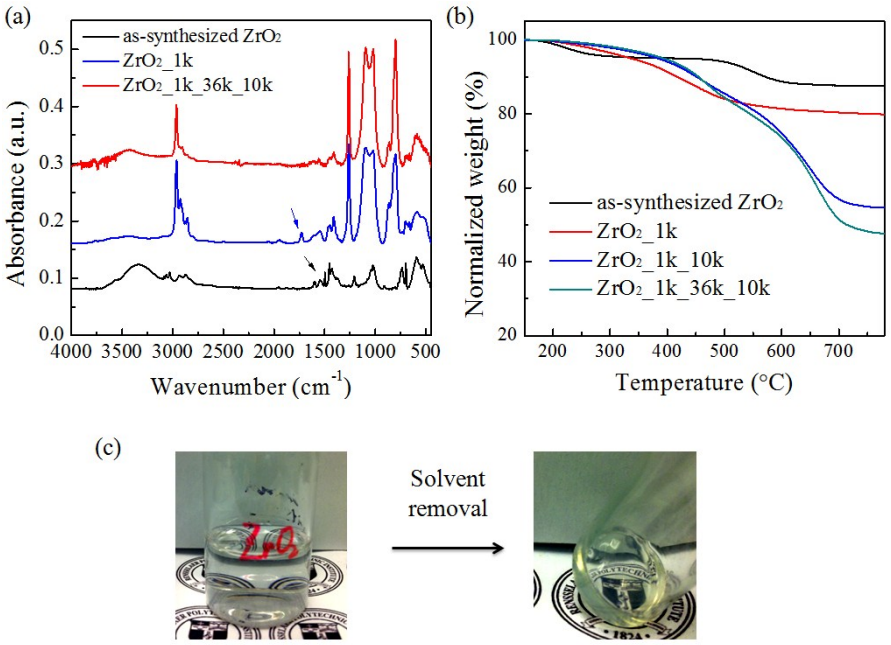

Figure S2 (a) FTIR spectra and (b) TGA curves of ZrO_2 nanoparticle at different grafting steps. (c) Photographs of grafted NP sample before and after solvent removal.

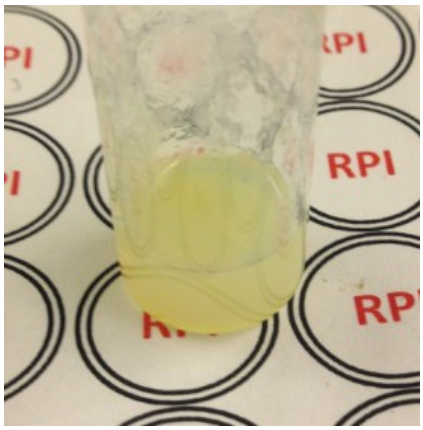

Figure S3. Photograph showing cloudy TiO_2_36k_10k nanoparticle packing after solvent removal.

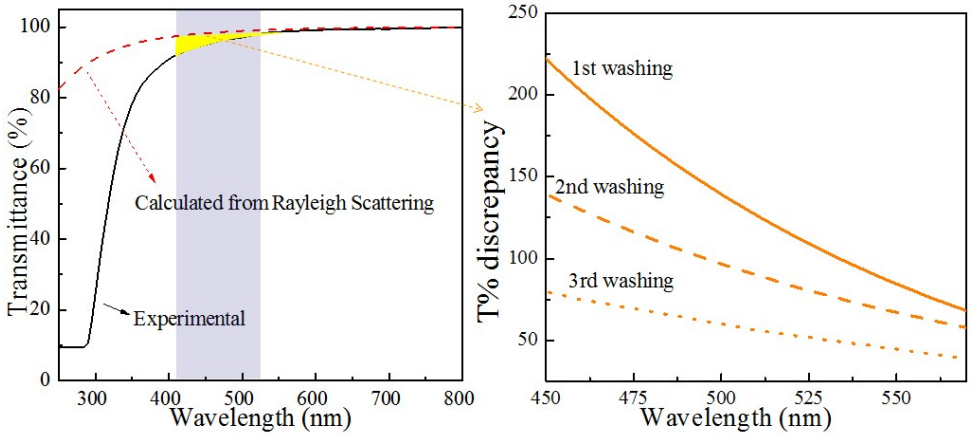

Figure S4. (a) UV-vis transmittance spectra of ZrO_2_1k_10k NP thin film (~0.5 mm) obtained from experiment (solid line) and calculation from Rayleigh scattering equation (dashed line). The yellow area was used to characterize blue absorption. (b) The gradual reduction in blue absorption with repeating washing process of the nanocomposite.

In order to verify whether there is absorption of blue light in ZrO_2_1k_10k sample, we compare its experimental transmittance spectrum with a transmittance spectrum calculated from the Rayleigh scattering equation. As show in Figure S4 (a), the transmittance spectrum should follow the prediction from the Rayleigh scattering equation assuming no absorption (dashed orange line).[6] However, there is transmittance discrepancy between the experimental data and the calculated curve starting from ~520 nm, which confirms the existence of blue absorption, leading to reduced light extraction enhancement of the blue LED. The absorption of blue light is probably due to the yellow-colored small organic components absorbed on the

particle surfaces such as aromatic species, which could be produced during the high-temperature synthesis of the nanoparticles.[14] We attempted to quantitatively characterize the blue absorption by subtracting the integrated area below the experimental transmittance spectrum from that of the theoretical spectrum, and the transmittance discrepancy were plotted against wavelength (Figure S4 (b)). It was found that by repeating the washing procedure using methanol while backfilling the grafted nanoparticle with shorter brush to prevent aggregation, these yellow organic components were gradually replaced.

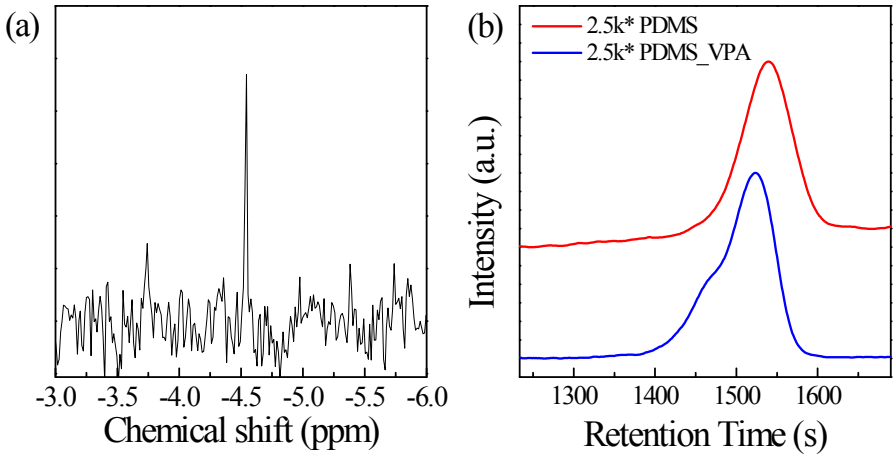

Figure S5. (a) ^{31}P NMR and (b) GPC analysis of the 2.5k* cross-linkable brush synthesized through hydrosilylation reaction.

As shown in **Figure S6** (a), compared to the physically adsorbed hydroxyl and organic volatiles, 10k* and 2.5k* cross-linkable brushes bind strongly with ZrO_2 NPs through a M - O - P bond, and correspond to the weight loss stage at much higher temperatures. This result is consistent with previous observations for flowable "matrix-free" nanocomposites (ZrO_2_1k and ZrO_2_1k_36k_10k). The FTIR spectrum of ZrO_2_1k_10k*_2.5k* demonstrated the 3046 and 1640 cm^{-1} peaks attributable to the C-H stretching and C=C stretching of the vinyl group.[5]

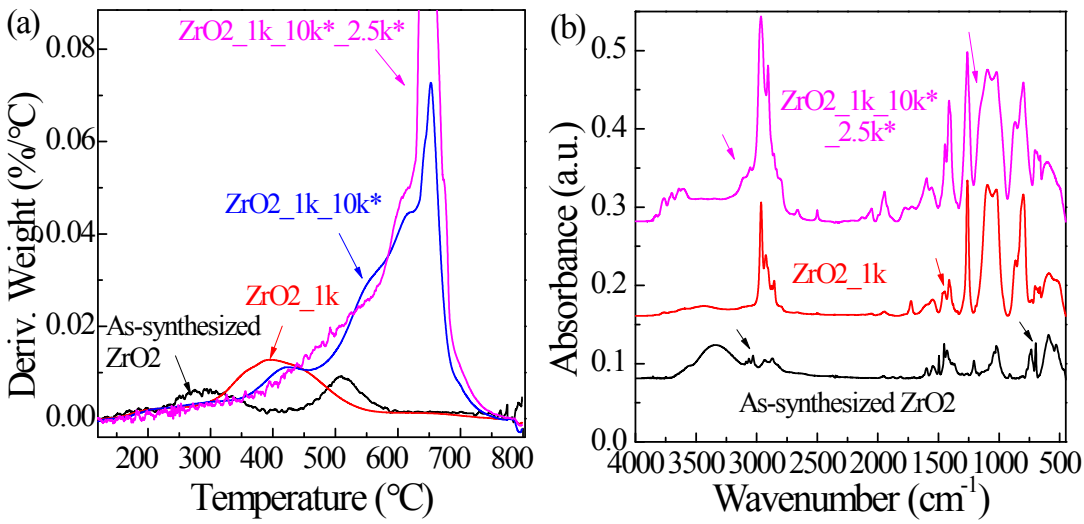

Figure S6. (a) Derivative weight loss and (b) FTIR comparison of as-synthesized and modified cross-linkable ZrO_2 NPs.

Instrumentations: The as-synthesized ZrO_2 nanoparticles were characterized by a PANalytical X'Pert Pro Diffractometer, solution Nuclear Magnetic Resonance (NMR, 500 MHz, $CDCl_3$), and a JEOL-2010 transmission electron microscope (TEM). Powder X-ray diffraction (XRD) patterns were recorded using Cu Kα radiation (λ=0.154 nm at 40 mA and 45 kV) over the 2θ range of 20 to 100° at a scan rate of 0.01°/min. The nanoparticle solution was dropped onto a carbon supported copper grid and dried in the hood overnight for TEM observation. The nanoparticle core fraction was determined by thermogravimetric analysis (TGA) using TA Instruments TGA-Q50. The grafted nanoparticles were characterized by a FT-IR Spectrophotometer (Perkin Elmer Spectrum One) scanning from 450 to 4000 cm^{-1} with a resolution of 4 cm^{-1} for 10 scans. Refractive index of neat silicone and nanocomposites was measured on a variable angle spectroscopic ellipsometer (VASE, J.A. Woollam Co., Inc., Lincoln, NE) at three different incident angles (65, 70, and 75°). The samples were spin-coated on a Si wafer, and the measured results were fitted with the Cauchy model with a typical mean square error less than 5. The transmittance spectra of the sample-casted glass slides were measured with a Perkin-Elmer Lambda 950 UV/vis/NIR spectrophotometer. The spectral fluxes measurements of encapsulated LEDs were carried out in a 0.5 meter

integrating sphere (Labsphere). The rheological experiments were carried out on a Rheometrics mechanical spectrometer (ARES cone & plate; TA Instruments®, USA) using a parallel-plate geometry (R=8 mm).

1. R. Vacassy, C. Guizard, V. Thoraval and L. Cot, *J. Membr. Sci.*, 1997, **132**, 109-118.
2. G. Garnweitner, L. M. Goldenberg, O. V. Sakhno, M. Antonietti, M. Niederberger and J. Stumpe, *Small*, 2007, **3**, 1626-1632.
3. V. Bansal, D. Rautaray, A. Ahmad and M. Sastry, *J. Mater. Chem.*, 2004, **14**, 3303-3305.
4. G. Lucovsky and G. Rayner, *Appl. Phys. Lett.*, 2000, **77**, 2912-2914.
5. S. Zhou, G. Garnweitner, M. Niederberger and M. Antonietti, *Langmuir*, 2007, **23**, 9178-9187.
6. P. Tao, Y. Li, R. W. Siegel and L. S. Schadler, *J. Appl. Polym. Sci.*, 2013, **130**, 3785–3793.
7. P. Tao, Y. Li, A. Rungta, A. Viswanath, J. Gao, B. C. Benicewicz, R. W. Siegel and L. S. Schadler, *J. Mater. Chem.*, 2011, **21**, 18623-18629.
8. M. Kobayashi, R. Matsuno, H. Otsuka and A. Takahara, *Sci. Tech. Adv. Mater.*, 2006, **7**, 617-628.
9. C. K. Wu, K. L. Hultman, S. O'Brien and J. T. Koberstein, *J. Am. Chem. Soc.*, 2008, **130**, 3516-3520.
10. D. Dukes, Y. Li, S. Lewis, B. Benicewicz, L. Schadler and S. K. Kumar, *Macromolecules*, 2010, **43**, 1564-1570.
11. T. Wu, K. Efimenko, P. Vlcˇek, V. Šubr and J. Genzer, *Macromolecules*, 2003, **36**, 2448-2453.
12. N. Nair, N. Wentzel and A. Jayaraman, *J. Chem. Phys.*, 2011, **134**, 194906.

13. H. Brouwers, *Phys. Rev. E*, 2007, **76**, 041304.

14. M. Niederberger and G. Garnweitner, *Chem. Eur. J.*, 2006, **12**, 7282-7302.